

## The fate of the merger remnant in GW170817 and its imprint on the jet structure

ARIADNA MURGUIA-BERTHIER,<sup>1,2</sup> ENRICO RAMIREZ-RUIZ,<sup>1,2</sup> FABIO DE COLLE,<sup>3</sup> AGNIESZKA JANIUK,<sup>4</sup> STEPHAN ROSSWOG,<sup>5</sup> AND WILLIAM H. LEE<sup>6</sup>

<sup>1</sup>*Department of Astronomy and Astrophysics, University of California, Santa Cruz, CA 95064, USA*

<sup>2</sup>*DARK, Niels Bohr Institute, University of Copenhagen, Blegdamsvej 17, 2100 Copenhagen, Denmark*

<sup>3</sup>*Instituto de Ciencias Nucleares, Universidad Nacional Autónoma de México, A. P. 70-543, 04510 CDMX, México*

<sup>4</sup>*Centrum Fizyki Teoretycznej PAN Al. Lotników 32/46, 02-668 Warsaw, Poland*

<sup>5</sup>*Astronomy and Oskar Klein Centre, Stockholm University, AlbaNova, SE-10691, Stockholm, Sweden*

<sup>6</sup>*Instituto de Astronomía, Universidad Nacional Autónoma de México, A. P. 70-264, 04510 CDMX, México*

### ABSTRACT

The first neutron star binary merger detected in gravitational waves, GW170817 and the subsequent detection of its emission across the electromagnetic spectrum showed that these systems are viable progenitors of short  $\gamma$ -ray bursts (sGRB). The afterglow signal of GW170817 has been found to be consistent with a structured GRB jet seen off-axis, requiring significant amounts of relativistic material at large angles. This trait can be attributed to the interaction of the relativistic jet with the external wind medium. Here we perform numerical simulations of relativistic jets interacting with realistic wind environments in order to explore how the properties of the wind and central engine affect the structure of successful jets. We find that the angular energy distribution of the jet depends primarily on the ratio between the lifetime of the jet and the time it takes the merger remnant to collapse. We make use of these simulations to constrain the time it took for the merger remnant in GW170817 to collapse into a black hole based on the angular structure of the jet as inferred from afterglow observations. We conclude that the lifetime of the merger remnant in GW170817 was  $\approx 0.8 - 0.9$ s, which, after collapse, triggered the formation of the jet.

### 1. INTRODUCTION

The gravitational wave event GW170817 (Abbott et al. 2017), that was accompanied by the detection of emission across the electromagnetic spectrum (Coulter et al. 2017), demonstrated that neutron star binary mergers are the sources of short  $\gamma$ -ray bursts (sGRBs; Eichler et al. 1989; Narayan et al. 1992), or at least a subset of them.

From the unusually faint nature of GRB 170817A it was initially argued that this event belonged to a class of intrinsically sub-energetic sGRBs (Margutti et al. 2018), but as more is being learned about GRB 170817A, the more it appears like the afterglow emission is instead consistent with the neutron star merger having triggered a typical, powerful sGRB seen at an angle of about a few times the opening angle of the central jet (Lazzati et al. 2017; Murguia-Berthier et al. 2017a; Duffell et al. 2018; Lamb et al. 2018, 2019; Mooley et al. 2018; Wu & MacFadyen 2018).

A question that has remained largely unanswered so far is what determined the typical structure of the jet in GRB 170817A, which is required not to have sharp edges but wings of lower kinetic energy and Lorentz factors that extend to large angles (Lazzati et al. 2017; Duffell et al. 2018; Bromberg et al. 2018; Granot et al. 2018; Lamb & Kobayashi 2018; Kathirgamaraju et al. 2018; van Eerten et al. 2018; Gill et al. 2019a; Lamb et al. 2019; Lazzati & Perna 2019; Lazzati

et al. 2020). This in turn might be attributed to the interaction of the jet interaction with a dense surrounding gas distribution, quite possibly the wind emanating from the merger remnant.

A trait of the jet-wind interaction is that there can be an exchange of linear momentum with the neighboring wind, even if there is minimal exchange of baryons (Lee & Ramirez-Ruiz 2007). As a result, the jet itself is then likely to develop a velocity profile so that different portions move with different Lorentz factors (Aloy et al. 2005; Rosswog & Ramirez-Ruiz 2002). This implies that an observer could infer a value for the Lorentz factor that depends upon the inclination of the line of sight to the jet axis. In this case, the early afterglow emission of GRB 170817A would be naturally produced by the deceleration of the lower Lorentz factor material moving along our line of sight (Lamb & Kobayashi 2018).

We already know that winds are a prominent feature of neutron star merger remnants and are accompanied by prodigious mass loss (Lee & Ramirez-Ruiz 2007; Rosswog & Ramirez-Ruiz 2003; Perego et al. 2014). This is not on the face of it the most advantageous environment to produce a baryon-starved jet. Studies of sGRB jets (Eichler et al. 1989; Narayan et al. 1992; Lee & Ramirez-Ruiz 2007) are thus increasingly invoking the collapse of the remnant to a black

hole, which neatly avoids the problem of catastrophic mass pollution close to the jet creation region, and allows the terminal jet Lorentz factors to be large. These issues motivate our study of the interaction between the jet and the pre-collapse wind through which the jet is expected to propagate. This jet-outflow interaction could turn out to be key for interpreting the observed properties of GRB 170817A.

The pre-burst gas distribution depends on how the binary neutron star merger loses mass. As the binary coalesces, various mechanisms can transport angular momentum and dissipate energy in the newly formed remnant (Baiotti et al. 2008), giving rise to significant mass-loss (Lee & Ramirez-Ruiz 2007). One important transport mechanism is the neutrino-driven wind (NDW) (Rosswog & Ramirez-Ruiz 2003; Dessart et al. 2009; Perego et al. 2014), as copious amounts of neutrinos are created in the merger remnant. The high flux of neutrinos will interact with matter in and around the merger remnant, driving a baryon loaded wind. Another important mechanism is energy and angular momentum transport mediated by magnetic fields. Even an initial weak field can destabilize the merger remnant via the so called magneto-rotational instability (e.g. Ruiz et al. 2019).

This merger remnant is assumed to be unstable and its subsequent collapse to a black hole is assumed to trigger a relativistic jet (McKinney et al. 2012; Ruiz et al. 2016; van Eerten et al. 2018; Ruiz et al. 2019). This is thought to be the case for GRB 170817, since a long-lived remnant is difficult to reconcile with observations (e.g. Ciolfi 2020). In this case, the jet will then unavoidably interact with the pre-collapse winds.

The interaction of the wind has a decisive effect in shaping the jet (Murguia-Berthier et al. 2014, 2017b). What is more, there are instances in which the wind can be dense enough to become a death trap for the jet, choking the outflow and rendering sGRB production unsuccessful. Therefore it is important to understand how the properties of the wind and central engine affect the structure of the jet. A key property of the binary neutron star merger is the time it takes for the remnant to collapse into a black hole, which is directly linked to the lifetime of the wind. Thus, by understanding how the interaction with the wind can alter the jet structure, one can constrain the lifetime of this remnant.

In this *Letter* we perform special relativistic simulations to study how the jet structure is affected by the neutrino driven wind and the magnetized disk outflow. We also explore how the time delay between collapse and jet triggering affects the structure of the jet. We use these simulations to set a limit on the delay time of GW170817 based on the angular structure of the jet that is inferred from afterglow observations.

## 2. JET AND WIND INTERACTION

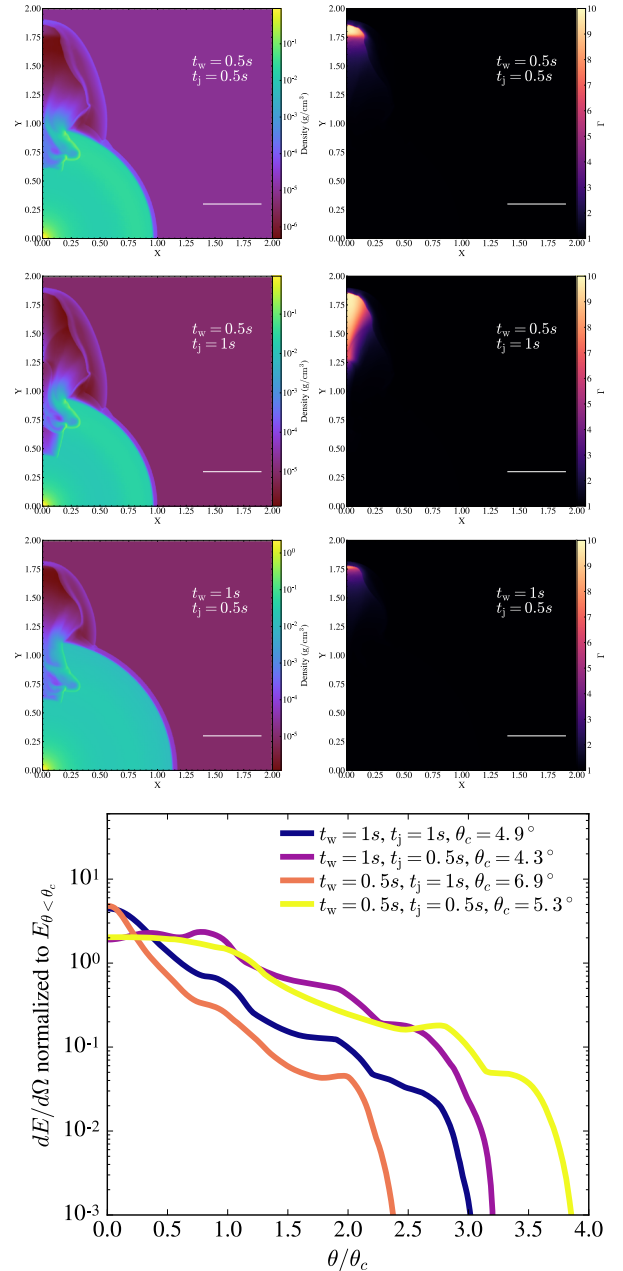


**Figure 1.** *Top Panels:* Density (*Left*) and Lorentz factor (*Right*) profiles of simulations of the interaction of a relativistic jet with a spherical wind. The bar corresponds to  $1.5 \times 10^{10}$  cm. Calculations were done in 2D spherical coordinates using an adaptive grid of size  $l_r = 6 \times 10^{10}$  cm,  $l_\theta = \pi/2$  with  $100 \times 40$  initial cells and five levels of refinement resulting in a maximum resolution of  $3.75 \times 10^7$  cm. The luminosity is  $L_j = 1 \times 10^{50}$  erg/s, the initial Lorentz factor  $\Gamma = 10$ , and the initial half-opening angle  $\theta_0 = 10^\circ$ . The wind has an  $\dot{M} = 10^{-3} M_\odot/s$  and  $v_w = 0.3c$ . Different simulations assume different collapse times and jet lifetimes. The simulations were run up to 4s. The *Top* and *Middle* snapshots were taken after 2.75s while the *Bottom* one was taken after 3.25s. *Bottom Panel:* Energy per unit angle of the resulting jet. The time is the same as the above panel. The energy is normalized to the total energy in the core of the jet.

### 2.1. Numerical method and Setup

Our simulations follow the setup described in Murguia-Berthier et al. (2014, 2017b). They are performed in 2D axisymmetric coordinates using *Mezcal*, an adaptive mesh refinement code that solves the equations of special relativistic hydrodynamics. A description of the code and a number of benchmark tests can be found in De Colle et al. (2012a,b).

The setup begins with the injection of a wind, lasting for a time  $t_w$ . This  $t_w$  is directly related to the time it takes the merger remnant to collapse to a black hole. After that time, the density of the wind is assumed to decrease as  $t^{-5/3}$ , and a jet is introduced. Motivated by GRMHD simulations (McKinney et al. 2012; Ruiz et al. 2016, 2019), the jet is assumed to initially have a top-hat structure characterized by a half-opening angle  $\theta_j$ , a luminosity  $L_j$  and a Lorentz factor of  $\Gamma = 10$  that are constant with angle. The central engine powers the jet for a time  $t_j$ .

Three different wind distributions as a function of angle are simulated. The first is a constant uniform spherical wind (Murguia-Berthier et al. 2014). The second is a non-spherical latitudinal distribution in density and velocity (Murguia-Berthier et al. 2017b), whose distribution is based on the global simulations of Perego et al. (2014), accurately representing the neutrino-driven wind from the merger remnant. Additionally, we have included a density profile of a magnetized wind outflow based on the simulations by Janiuk (2019). The density profiles in both cases are similar, they are denser in the equator and progressively lighter in the polar region. The density as a function of angle is obtained by averaging the latitudinal profiles at the end of the simulations (Perego et al. 2014; Janiuk 2019). For comparison, the ratio of the density in the polar region ( $\theta = 0^\circ$ ) versus that in the equator ( $\theta = 90^\circ$ ) is  $\rho_{\text{eq}}/\rho_{\text{pl}} \approx 10^2$  for the NDW and  $\rho_{\text{eq}}/\rho_{\text{pl}} \approx 1.5 \times 10^3$  for the magnetized outflow.

### 2.2. Results

Initially, the jet is unable to move the wind material at a speed comparable to its own and thus is decelerated. As the jet propagates in the wind a bow shock runs ahead of it, which both heats material and causes it to expand sideways (Ramirez-Ruiz et al. 2002; Bromberg et al. 2011; Salafia et al. 2020). The parameter that controls the evolution of the jet interacting with the wind is (Bromberg et al. 2011):

$$\tilde{L} = \frac{\rho_j h_j \Gamma_j}{\rho_w}, \quad (1)$$

where  $\rho$  is the density,  $h$  is the enthalpy,  $\Gamma$  is the Lorentz factor and the subscripts  $j, w$  refer to the jet and the wind, respectively. Once the jet breaks free from the wind, though, the evolution becomes self-similar and its structure remains unchanged.

The interaction of the jet with the wind will result in an angular redistribution of the jet's energy, which can naturally

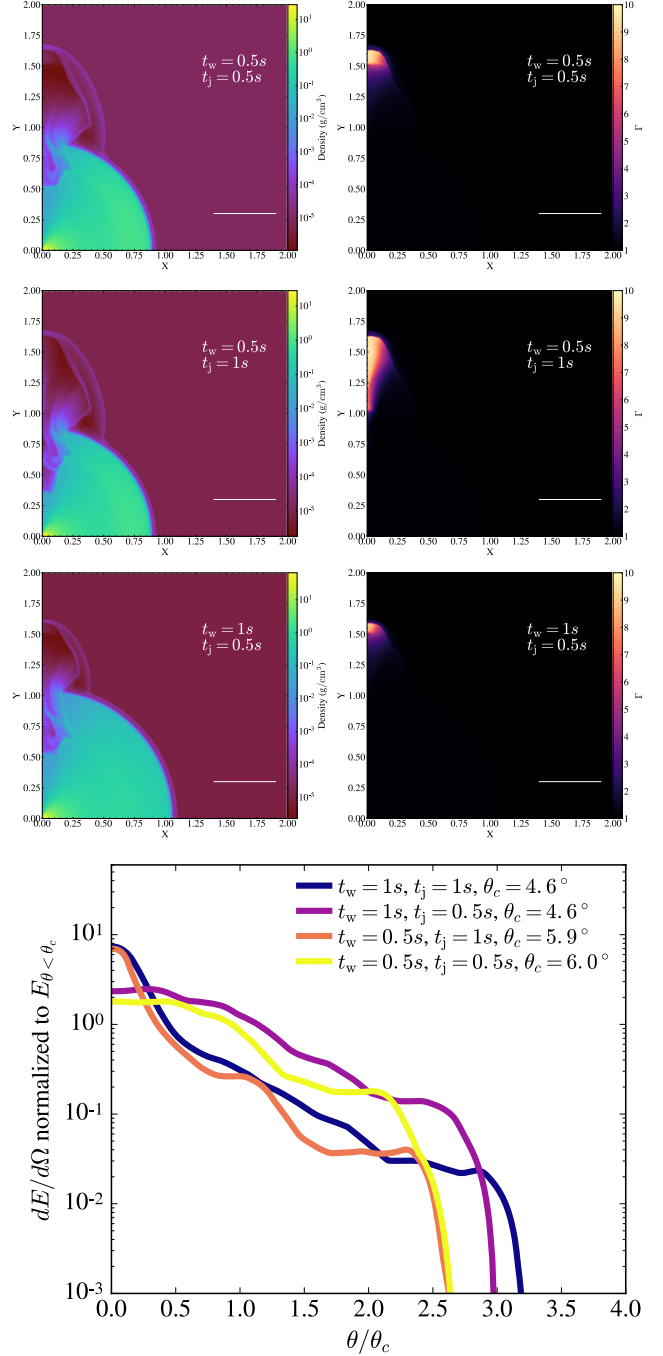


**Figure 2.** *Top Panel:* Density (*Left*) and Lorentz factor (*Right*) profiles of simulations of the interaction of the relativistic jet with a neutrino-driven wind. Shown is a  $1.5 \times 10^{10}$  cm scale bar. The resolution, as well as the properties of the jet are the same as in Fig 1. The *Top* and *Middle* Panels show snapshots after 2.5s while 3s for the *Bottom* Panel. The wind has a mass loss rate of  $\dot{M} = 10^{-3} M_\odot/\text{s}$  in the polar region and a velocity of  $v_w = 0.3c$ . *Bottom Panel:* Energy per unit angle of the jet after its propagation. The time is the same as the above panel. The energy is normalized to the energy in the core.

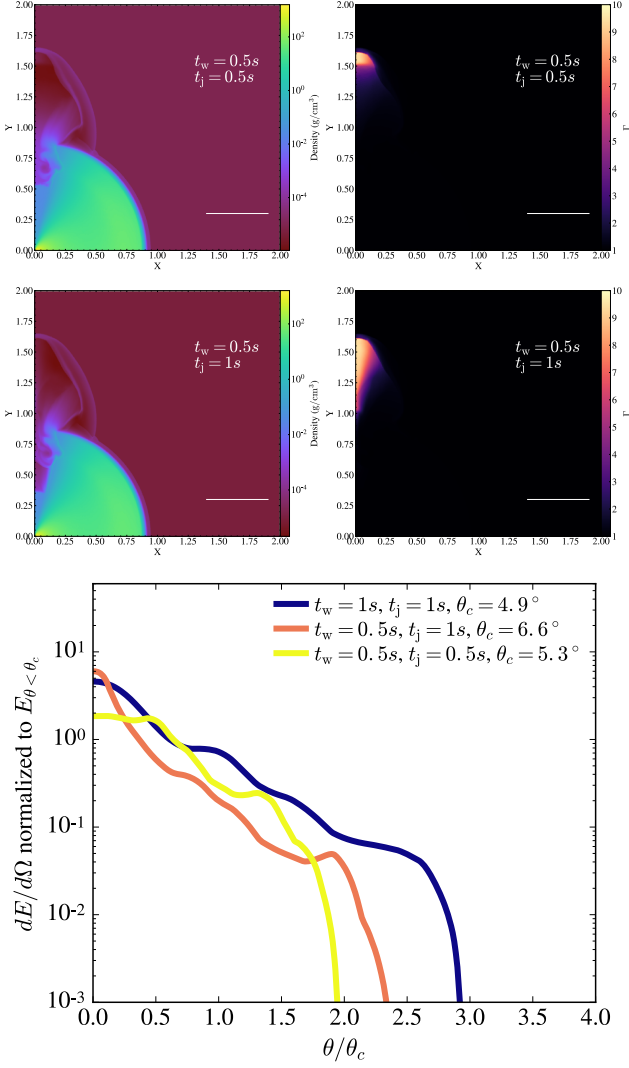


**Figure 3.** *Top Panel:* Density (*Left*) and Lorentz factor (*Right*) profiles of simulations of the interaction of a relativistic jet with a magnetized wind based on Janiuk (2019). Shown is a  $1.5 \times 10^{10}$  cm scale bar. The resolution, as well as the properties of the jet are the same as in Fig 1. The wind has a mass loss rate of  $\dot{M} = 10^{-3} M_{\odot}/s$  in the polar region and  $v_w = 0.3c$ . The *Top* and *Middle* Panels correspond to a simulation time of 2.5s. The simulation corresponding to  $t_w = 1s$ ,  $t_j = 0.5s$  is not shown as the wind in that case is dense enough to choke the jet, rendering the sGRB unsuccessful. *Bottom Panel* Energy per unit angle of the jet resulting from the simulations. The time is the same as the above panel. The energy is normalized to the energy in the core.

give rise to a different afterglow lightcurve than the one from the original top-hat structure (Lazzati et al. 2017; Duffell et al. 2018; Bromberg et al. 2018; Granot et al. 2018; Lamb & Kobayashi 2018; Kathirgamaraju et al. 2018; van Eerten et al. 2018; Lamb et al. 2019; Salafia et al. 2019; Lazzati et al. 2020; Gottlieb et al. 2020). In what follows, we explore how the properties of the pre-collapse wind affect the structure of

a jet propagating through it. We perform different simulations, for a given wind profile, by altering the lifetime of the wind ( $t_w$ ), which is directly related to the time it takes the merger remnant to collapse to a black hole. We also changed the duration of the jet ( $t_j$ ), which is the characteristic time the central engine is active and is broadly related to the duration of the event. We show our results in Figures 1, 2 and 3, where we plot the density and Lorentz factor distributions of jets propagating through a spherical wind, a neutrino-driven wind and a magnetically ejected wind, respectively.

Common to all calculations is the altering of  $t_w$  and  $t_j$ . Also shown is the final angular distribution of the energy in the relativistic jet. In all simulations we define the core angle of the jet, after its propagation, as the angle where the Lorentz factor of the jet decreases by a factor of 2 from its initial value. The resulting core angles range from  $4.5^\circ$  to  $7^\circ$ , which are similar to the values quoted in the literature (Lyman et al. 2018; D’Avanzo et al. 2018; Troja et al. 2018; Salafia et al. 2019; Ghirlanda et al. 2019; Lazzati et al. 2020). The final angular distribution of Lorentz factor is fairly gaussian.

In the case of a spherical wind, as shown in Figure 1, the jet, originally a top-hat, spreads laterally thus resulting in a structured jet. In the other cases, shown in Figure 2 and Figure 3, the jet escapes along the direction of least resistance, which is along the rotation axis of the merger remnant. Despite the fact that there is a decrease in confinement along the polar region, the difference in the final structure of the jet is not highly sensitive to the exact structure of the wind. In Figure 3, we show for comparison a simulation of a jet propagating in the magnetized wind. In that case, the wind density is higher, which makes it easier for the jet to get choked. This is indeed the case for the  $t_w = 1s$  and  $t_j = 0.5s$  simulation of the jet propagating in the denser magnetized wind. For a jet to be successful in that particular case, the central engine must be active for longer and/or produce a higher jet luminosity (Murguia-Berthier et al. 2017b).

In addition to the density structure of the wind, the ratio  $t_w/t_j$  plays a decisive effect on the appearance of a jet propagating through a dense wind. This is because it determines the time the jet resides within the interaction region (as governed by  $\bar{L}$ ) which in turn regulates the amount of relativistic material that is shocked. The importance of this ratio can be clearly seen in the *Bottom* panels of Figures 1, 2 and Figure 3. If the delay time is larger or comparable to the duration of the jet, the time it takes for the jet to break free from the wind is augmented. In this case, the afterglow emission would be dominated by the emission of the laterally spreading relativistic material, which is located at larger angles relative to the rotation axis of the merger remnant.

On the other hand, if the jet produced by the accretion onto the black hole maintains its energy for much longer than it takes the jet head to reach the edge of the wind, the core of

the relativistic jet would contain substantially more energy than the off-axis material, so that it is likely to dominate the afterglow flux even after expanding for a longer time. The detection of varying afterglow signatures would be a test of the neutron star merger model; and the precise inference of the angular structure of the jet may help constrain the properties of the wind and the lifetime of the merger remnant.

### 3. RELEVANCE TO GW170817

Several groups (Lazzati et al. 2018; Margutti et al. 2018; Lyman et al. 2018; D’Avanzo et al. 2018; Troja et al. 2018; Ghirlanda et al. 2019; Salafia et al. 2019; Lazzati et al. 2020) have studied the origin of the afterglow emission of GW170817 and concluded that it can be explained by invoking a model where the sGRB was successful and the observer lies off axis to the jet. A common feature of all models is the need for significant amount of energy at larger angles, which as we have argued here can be a natural consequence of the interaction of the jet with the pre-collapse wind. In this section we endeavor to compare our simulation results to the jet models constructed for GW170817.

Various groups inferred different energy distributions for the jet. In Figure 4 we compare their best fit models for the jet profiles with those obtained from our simulations. The results from our simulations are in broad agreement with the energy distributions derived from afterglow observations. We thus conclude that the structure of an initially top-hat jet can be modified by its interaction with the pre-collapse wind and, after the jet emerges from this region, can have a structure that closely resembles the one deduced for GW170817. So in these models the  $\gamma$ -rays would be restricted to a narrow beam, even though outflow with a more moderate Lorentz factor, which is relevant to the afterglow emission, is spread over a wider range of angles.

While the properties of the pre-collapse wind have an important effect on the appearance of a jet propagating through it (Figure 4), our calculations suggest that  $t_w/t_j$  is the essential parameter that controls how much relativistic energy is distributed at large angles. As seen in the *Bottom* panel in Figure 4, variations in the jet power and on the mass loss rate are observed to have only mild effects on the angular structure of the resulting jets.

Figure 5 illustrates the effect of varying  $t_w/t_j$  for jets propagating within the three different wind profiles we have considered in this study. It shows how the ratio of the energy contained in the core of the jet to that residing outside it increases as  $t_w/t_j$  augments. In the case of a successful breakthrough, the resultant jet structure could result in an afterglow signature similar to that observed in GW170817 if the time it took for the merger remnant to collapse is similar to the observed duration of the event.

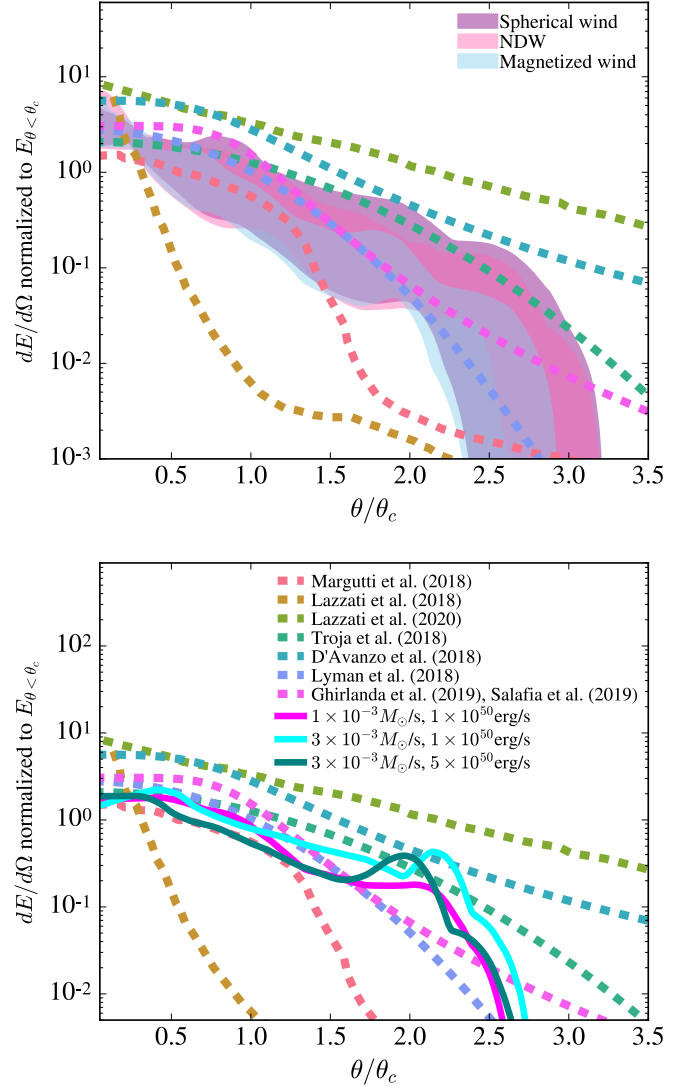


**Figure 4.** Comparison of different jet profiles used to model the emission of GW170817 with those obtained from our simulations. *Top Panel:* Jet profiles for the various winds at a fixed jet luminosity of  $10^{50}$  erg/s but varying  $t_w/t_j = 0.5, 1, 2$ . The dotted lines show the jet profiles inferred for GW170817 and taken from Lazzati et al. (2018); Margutti et al. (2018); Lyman et al. (2018); D’Avanzo et al. (2018); Troja et al. (2018); Ghirlanda et al. (2019); Salafia et al. (2019); Lazzati et al. (2020). *Bottom Panel:* Jet profiles resulting from the interaction of a jet with a NDW. The solid lines show the jet profiles for the case where  $t_w = 0.5$ s and  $t_j = 0.5$ s. In magenta we plot the case with  $L_j = 10^{50}$  erg/s and  $\dot{M} = 10^{-3} M_\odot/s$ , which has  $\theta_c = 6^\circ$ . In cyan we plot the case with  $\dot{M} = 3 \times 10^{-3} M_\odot/s$ , which has  $\theta_c = 5.9^\circ$ . In teal we plot the case with  $L_j = 5 \times 10^{50}$  erg/s and  $\dot{M} = 3 \times 10^{-3} M_\odot/s$ , which has  $\theta_c = 7^\circ$ .

A constraint for  $t_w$  can be derived by requiring a successful jet (Murguía-Berthier et al. 2017b), which can be written as

$$t_w \lesssim t_j \frac{\beta_h - \beta_w}{\beta_w}, \quad (2)$$

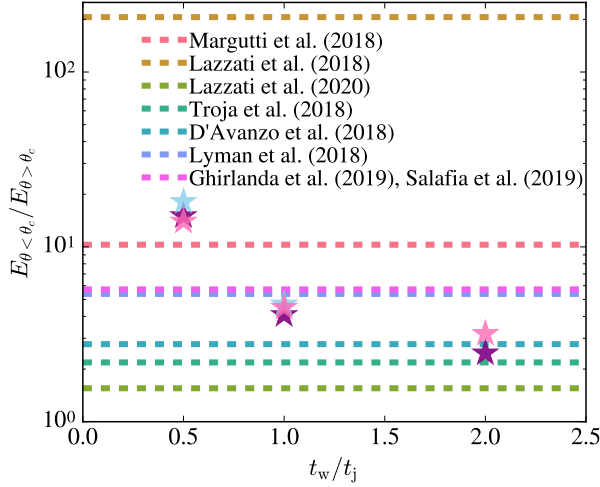


**Figure 5.** Comparison of the energy content in the jet’s core,  $E_{\theta < \theta_c}$ , with that stored in the wings,  $E_{\theta > \theta_c}$ . This ratio is plotted as a function of  $t_w/t_j$  for the three different wind profiles: a NDW (pink stars); a spherical wind (purple stars) and a magnetized wind (blue stars). The constant lines represent the same energy ratio taken from GW170817 jet models (Lazzati et al. 2018; Margutti et al. 2018; Lyman et al. 2018; D’Avanzo et al. 2018; Troja et al. 2018; Ghirlanda et al. 2019; Salafia et al. 2019; Lazzati et al. 2020).

where  $\beta_w = v_w/c$ ,  $\beta_h = v_h/c$  and the subscript  $h$  referring to the head of the jet. Making use of the commonly assumed values inferred for GW170817:  $E_{\gamma, \text{iso}} \approx 10^{52}$  erg,  $\theta_c \approx 5^\circ$  and  $t_j \approx 1.7$  s, we find that in order for the jet to be successful, the time delay for the remnant to collapse is constrained to  $t_w \lesssim 0.9$  s. This estimate is derived using the neutrino-driven wind profile.

This constraint can then be combined with the one derived in Figure 5, which shows that in order for our models to explain the afterglow observations of GW170817 we require  $t_w \gtrsim \frac{1}{2}t_j \gtrsim 0.8$  s. The condition of a successful jet combined with the angular structure requirements thus gives  $t_w \approx 0.8-0.9$  s.

This finding gives further credence to the idea that in the case of GW170817, the collapse into a black hole was indeed delayed. Yet this argument comes from a completely different line of reasoning than those given in the literature:

- Murguia-Berthier et al. (2017b) set a constraint for the collapse time  $t_w \lesssim 0.9$ s based on the condition of a successful jet (equation 2).
- Granot et al. (2017) set a constrain of  $t_w \lesssim 1$  s based on the expected lifetime of a hyper-massive NS.

- Metzger et al. (2018) set a constrain of  $t_w \approx 0.1-1$ s based on the amount of blue ejecta expected from a magnetized wind.
- Gill et al. (2019b) did a comprehensive analysis and estimated the collapse time to be  $t_w = 0.98^{+0.31}_{-0.26}$ s. They combined several constraints including the delay time between the gravitational wave and electromagnetic signal, a comparison on the observational mass of the blue ejecta and constraints based on a succesful jet.
- van Putten et al. (2019) obtain a limit of  $t_w \approx 0.67 \pm 0.3$ s based on observations of extended emission.
- Lazzati et al. (2020) favour the delay time to be around  $t_w < 1.1$ s by parameter space exploration of jet-wind interactions using an analytical formalism.

Our estimate for  $t_w \approx 0.8-0.9$ s, which is based on the angular structure of the jet as inferred from afterglow observations, is consistent with these various estimates.

Many binary neutron star mergers are thought to produce sGRBs when collapsing to black holes but some merger remnants may experience significant delays before collapsing. One expects various outcomes ranging from sGRBs with narrow beams from prompt collapse to structured jets with bright and weak sGRBs for longer collapse timescales. The properties of the afterglow signatures produced by successful and non-successful jets would provide a natural test to distinguish between these different progenitor avenues.

We thank R. Ciolfi, I. Mandel, L. Nativi, R. Margutti, W.-F. Fong, A. Batta, N. Lloyd-Ronning, C. Kilpatrick, R. Foley, G. Lamb, O. Bromberg, S.-C. Noble and G. Urrutia for useful discussions. E.R-R and A.M-B are supported by the Heising-Simons Foundation, the Danish National Research Foundation (DNRF132) and NSF (AST-1911206 and AST-1852393). A.M-B acknowledges support from a UCMEXUS-CONACYT Doctoral Fellowship and NASA TCAN award TCAN-80NSSC18K1488. S.R. acknowledges support by the Swedish Research Council (VR) under grants 2016- 03657\_3 and 2016-06012, the Swedish National Space Board under Dnr. 107/16 and by the Knut and Alice Wallenberg Foundation (KAW 2019.0112). F.D.C. and W.H.L. acknowledge support from the UNAM-PAPIIT grant AG100820. A.J. was supported by the grants no. 2016/23/B/ST9/03114 and 2019/35/B/ST9/04000 from the Polish National Science Center, and acknowledges computational resources of the Warsaw ICM through grant Gb79-9, and the PL-Grid through the grant grb3.

## REFERENCES

- Baiotti, L., Giacomazzo, B., & Rezzolla, L. 2008, *PhRvD*, 78, 084033
- Bromberg, O., Nakar, E., Piran, T., & Sari, R. 2011, *ApJ*, 740, 100
- Bromberg, O., Tchekhovskoy, A., Gottlieb, O., Nakar, E., & Piran, T. 2018, *MNRAS*, 475, 2971
- Ciolfi, R. 2020, *MNRAS*, 495, L66
- Coulter, D. A., Foley, R. J., Kilpatrick, C. D., et al. 2017, *Science*, 358, 1556
- D’Avanzo, P., Campana, S., Salafia, O. S., et al. 2018, *A&A*, 613, L1
- De Colle, F., Granot, J., López-Cámara, D., & Ramirez-Ruiz, E. 2012a, *ApJ*, 746, 122
- De Colle, F., Ramirez-Ruiz, E., Granot, J., & Lopez-Camara, D. 2012b, *ApJ*, 751, 57
- Dessart, L., Ott, C. D., Burrows, A., Rosswog, S., & Livne, E. 2009, *ApJ*, 690, 1681
- Duffell, P. C., Quataert, E., Kasen, D., & Klion, H. 2018, *ApJ*, 866, 3
- Eichler, D., Livio, M., Piran, T., & Schramm, D. N. 1989, *Nature*, 340, 126
- Ghirlanda, G., Salafia, O. S., Paragi, Z., et al. 2019, *Science*, 363, 968
- Gill, R., Granot, J., De Colle, F., & Urrutia, G. 2019a, *ApJ*, 883, 15
- Gill, R., Nathanail, A., & Rezzolla, L. 2019b, *ApJ*, 876, 139
- Gottlieb, O., Nakar, E., & Bromberg, O. 2020, arXiv e-prints, arXiv:2006.02466
- Granot, J., Gill, R., Guetta, D., & De Colle, F. 2018, *MNRAS*, 481, 1597
- Granot, J., Guetta, D., & Gill, R. 2017, *ApJL*, 850, L24
- Janiuk, A. 2019, *ApJ*, 882, 163
- Kathirgamaraju, A., Barniol Duran, R., & Giannios, D. 2018, *MNRAS*, 473, L121
- Lamb, G. P., & Kobayashi, S. 2018, *MNRAS*, 478, 733
- Lamb, G. P., Mandel, I., & Resmi, L. 2018, *MNRAS*, 481, 2581
- Lamb, G. P., Lyman, J. D., Levan, A. J., et al. 2019, *ApJL*, 870, L15
- Lazzati, D., Ciolfi, R., & Perna, R. 2020, arXiv e-prints, arXiv:2004.10210
- Lazzati, D., Deich, A., Morsony, B. J., & Workman, J. C. 2017, *MNRAS*, 471, 1652
- Lazzati, D., & Perna, R. 2019, arXiv e-prints, arXiv:1904.08425
- Lazzati, D., Perna, R., Morsony, B. J., et al. 2018, *Physical Review Letters*, 120, 241103
- Lee, W. H., & Ramirez-Ruiz, E. 2007, *New Journal of Physics*, 9, 17
- Lyman, J. D., Lamb, G. P., Levan, A. J., et al. 2018, *Nature Astronomy*, 2, 751
- Margutti, R., Alexander, K. D., Xie, X., et al. 2018, *ApJL*, 856, L18
- McKinney, J. C., Tchekhovskoy, A., & Blandford, R. D. 2012, *MNRAS*, 423, 3083
- Metzger, B. D., Thompson, T. A., & Quataert, E. 2018, *ApJ*, 856, 101
- Mooley, K. P., Deller, A. T., Gottlieb, O., et al. 2018, *Nature*, 561, 355
- Murguia-Berthier, A., Montes, G., Ramirez-Ruiz, E., De Colle, F., & Lee, W. H. 2014, *ApJL*, 788, L8
- Murguia-Berthier, A., Ramirez-Ruiz, E., Kilpatrick, C. D., et al. 2017a, *ApJL*, 848, L34
- Murguia-Berthier, A., Ramirez-Ruiz, E., Montes, G., et al. 2017b, *ApJL*, 835, L34
- Narayan, R., Paczynski, B., & Piran, T. 1992, *ApJL*, 395, L83
- Perego, A., Rosswog, S., Cabezón, R. M., et al. 2014, *MNRAS*, 443, 3134
- Ramirez-Ruiz, E., Celotti, A., & Rees, M. J. 2002, *MNRAS*, 337, 1349
- Rosswog, S., & Ramirez-Ruiz, E. 2002, *MNRAS*, 336, L7
- . 2003, *MNRAS*, 343, L36
- Ruiz, M., Lang, R. N., Paschalidis, V., & Shapiro, S. L. 2016, *ApJL*, 824, L6
- Ruiz, M., Tsokaros, A., Paschalidis, V., & Shapiro, S. L. 2019, *PhRvD*, 99, 084032
- Salafia, O. S., Barbieri, C., Ascenzi, S., & Toffano, M. 2020, *A&A*, 636, A105
- Salafia, O. S., Ghirlanda, G., Ascenzi, S., & Ghisellini, G. 2019, *A&A*, 628, A18
- Troja, E., Piro, L., Ryan, G., et al. 2018, *MNRAS*, 478, L18
- van Eerten, E. T. H., Ryan, G., Ricci, R., et al. 2018, arXiv e-prints, arXiv:1808.06617
- van Putten, M. H. P. M., Della Valle, M., & Levinson, A. 2019, *ApJL*, 876, L2
- Wu, Y., & MacFadyen, A. 2018, *ApJ*, 869, 55